

Initial clinical application of modified Dixon with flexible echo times: hepatic and pancreatic fat assessments in comparison with ^1H MRS

Roshan S. Livingstone · Paul Begovatz · Sabine Kahl · Bettina Nowotny · Klaus Straßburger · Guido Giani · Jürgen Bunke · Michael Roden · Jong-Hee Hwang

Received: 6 July 2013 / Revised: 30 October 2013 / Accepted: 6 November 2013 / Published online: 4 December 2013
© ESMRMB 2013

Abstract

Objects Hepatic and pancreatic fat content become increasingly important for phenotyping of individuals with metabolic diseases. This study aimed to (1) evaluate hepatic fat fractions (HFF) and pancreatic fat fractions (PFF) using ^1H magnetic resonance spectroscopy (MRS) and the recently introduced fast mDixon method, and to examine body fat effects on HFF and PFF, (2) investigate regional differences in HFF and PFF by mDixon.

Materials and methods HFF and PFF were quantified by mDixon with two flexible echo times and by single voxel ^1H MRS in 24 healthy subjects. The regional differences of PFF within the pancreas were assessed with mDixon. Abdominal visceral and subcutaneous fat was assessed by T1-weighted MRI at 3T.

Results Both methods correlated well for quantification of HFF ($r = 0.98$, $p < 0.0001$) and PFF ($r = 0.80$,

$p < 0.0001$). However, mDixon showed a higher low limit in HFF and PFF. PFF showed no regional differences using mDixon. In addition, both visceral and subcutaneous fat correlated with pancreatic fat, while only visceral fat correlated with liver fat, employing both ^1H MRS and mDixon.

Conclusion The novel and fast two-point mDixon exhibits a good correlation with the gold-standard ^1H MRS for assessment of HFF and PFF, with limited sensitivity for assessing lower fat content.

Keywords Fat quantification · Modified Dixon MRI · Proton MR spectroscopy · Liver and pancreas

Introduction

Over the last decade, exact fat quantification using magnetic resonance (MR) techniques has become relevant not only for clinical–experimental applications, but also for clinical medicine to diagnose non-alcoholic fatty liver (NAFL) and assess risk of insulin resistance and metabolic diseases. First, ^1H magnetic resonance spectroscopy (MRS) made it possible to identify intramyocellular fat content as a marker of insulin resistance [1], and later it became the gold standard for accurate quantification of hepatic fat content due to its high sensitivity [2–5]. Apart from ^1H MRS, MR imaging (MRI) techniques such as the Dixon method with two or three echo times have been applied for the rapid assessment of hepatic or/and pancreatic fat [2, 4, 6–12]. This imaging modality could be advantageous in obtaining regional information within an organ, when compared to single voxel ^1H MRS. Traditionally, the echo times of Dixon methods are chosen to be at in-phase (IP) and out-of phase (OP) between water and fat signals.

R. S. Livingstone · P. Begovatz · S. Kahl · B. Nowotny · M. Roden · J.-H. Hwang (✉)
Metabolic Imaging Group, Institute of Clinical Diabetology, German Diabetes Center at Heinrich-Heine University, Auf dem Hennekamp 65, 40225 Düsseldorf, Germany
e-mail: Jong-hee.hwang@ddz.uni-duesseldorf.de

K. Straßburger · G. Giani
Institute for Biometry and Epidemiology, German Diabetes Center, Düsseldorf, Germany

J. Bunke
Philips Healthcare, Hamburg, Germany

M. Roden
Department of Endocrinology and Diabetology, Heinrich-Heine University, Düsseldorf, Germany

J.-H. Hwang
Gachon University of Medicine and Science, Incheon, Korea

Further efforts have been made to improve IP/OP Dixon [9–12], such as for making echo time to be flexible. Recently, Eggers and others introduced a modified Dixon (mDixon), which allows both echo times to be flexible [13, 14]. However, this new Dixon method has not been validated against the gold standard, ^1H MRS, particularly for liver fat assessment.

More recently, quantification of pancreatic fat content also gained interest due to the important role of the pancreas in secreting the key glucose-regulating hormones, insulin and glucagon. However, extensive studies on pancreatic fat quantification are rare. Intrapancreatic fat content may not only be relevant as another ectopic fat compartment related to insulin sensitivity, but also because of the relevance of augmented local fat availability, which may impair insulin secretion by lipotoxicity [15]. Furthermore, Heni et al. [16] reported that pancreatic fat content negatively correlated with insulin secretion, while liver fat did not in the group of subjects with impaired fasting glycemia and/or glucose tolerance. It is still under debate whether ^1H MRS or a Dixon-based method is more suitable for the quantification of pancreatic intracellular fat, due to fundamental differences in anatomy and its smaller size than the liver [2]. Of note, the pancreas can allow extracellular fat infiltration within the tissue, possibly affecting fat quantification [2, 17–19]. While fat is mostly homogeneously distributed in the liver in nonobese subjects [8], fat distribution within the pancreas is rarely examined by noninvasive imaging modality, except in one publication to date [16].

Finally, liver fat correlates well with abdominal visceral adipose tissue (VAT) [4, 20–24], whereas there were conflicting reports on the association of pancreatic fat and VAT [18, 20, 21]. But this has never been examined by employing different methods in the same population, which would help to minimize the ambiguity stemming from the systematical errors of a method.

Thus, the aims of this study were to (1) quantify and compare hepatic and pancreatic fat content using ^1H MRS and fast mDixon with two flexible echo times, (2) investigate the regional difference in pancreas and liver fat content using the mDixon, and (3) examine the impact of body fat content, particularly VAT and subcutaneous adipose tissue (SAT), on liver and pancreatic fat using both methods.

Materials and methods

Volunteers

Twenty-four healthy subjects (12 males and 12 females; mean age of 52.6 ± 18.0 years; mean body mass index

(BMI) of $25.8 \pm 5.0 \text{ kg/m}^2$) participated in the MR examinations after giving informed and written consent to the protocol, which had been approved by the local review board. None of subjects was diagnosed with liver or pancreatic diseases or dysfunctions.

Instrumentation

All measurements were performed on a 3.0-T MR scanner using a 16-channel Torso XL phased-array receiver coil (eight elements in anterior; eight elements in posterior; 40 cm of coverage in the head–foot direction) or body coil (Achieva X-series, Philips Healthcare, Best, The Netherlands). Body fat was measured using the built-in quadrature body coil on the 3.0-T scanner.

^1H MRS for hepatic and pancreatic fat measurements

Localizer for ^1H MRS for liver: All measurements were performed using a 16-channel torso SENSE coil. Prior to liver and pancreatic fat measurements, scout images for the liver ^1H MRS were taken using turbo spin echo (TSE, single-shot, repetition time (TR)/echo time (TE) = 2,080/80 ms, slice thickness 4 mm/gap 1 mm) to confirm the anatomical location of liver (Fig. 1a).

Localizer for ^1H MRS for pancreas: Since it was not easy to clearly identify pancreas with low resolution conventional MRI, three-dimensional (3D) fast mDixon sequence was employed (Fig. 1c) (spatial resolution: $1.7 \times 1.6 \times 1.7 \text{ mm}^3$) in a short acquisition time (17 s).

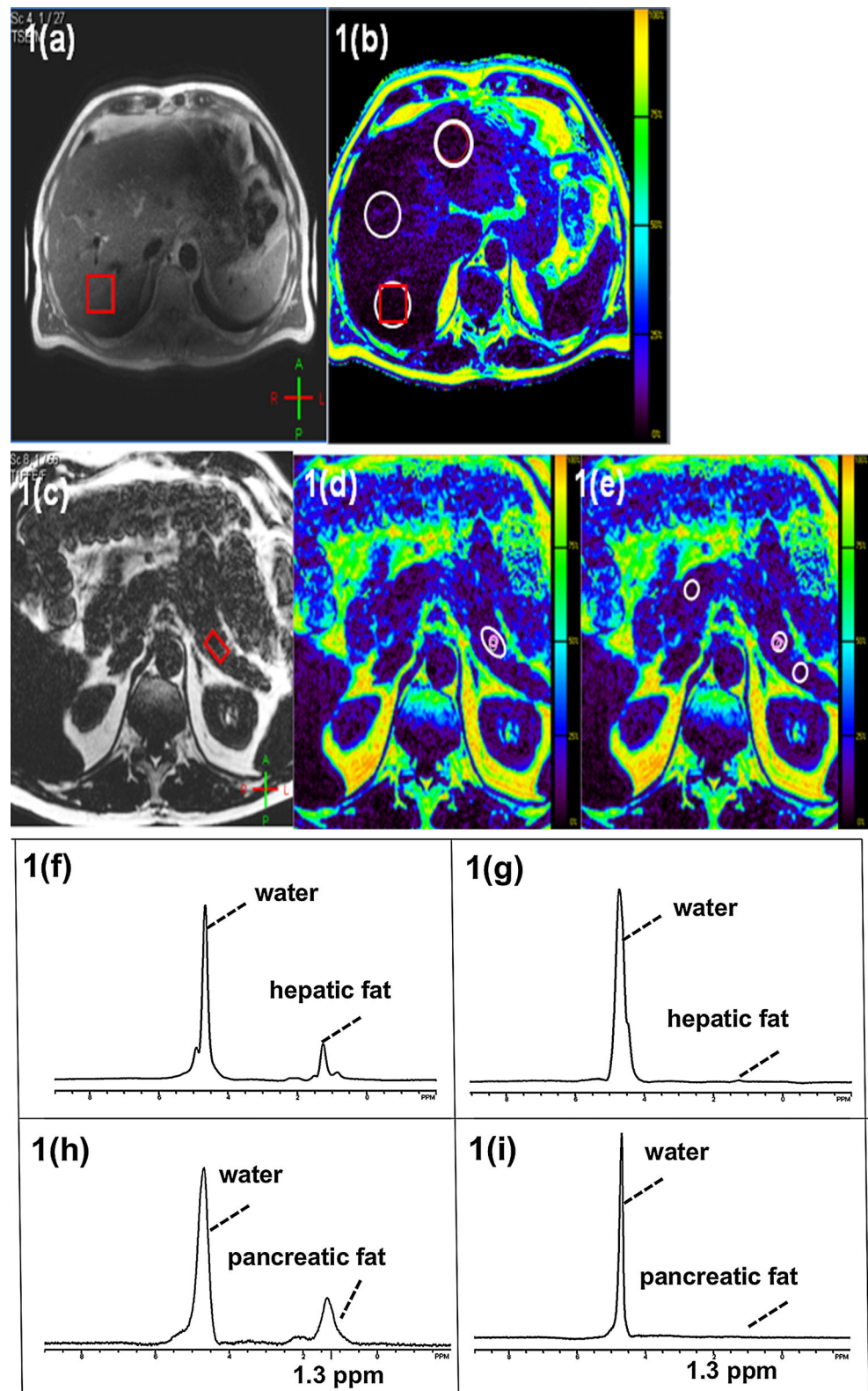
^1H MRS acquisition: for ^1H MRS, one location for liver and pancreas, respectively, was measured employing stimulated echo acquisition mode (STEAM) sequence [TR/TE/mixing time(TM) = 4,000/10/16 ms; number of scans (NS) = 32] using the same 16-channel SENSE coil as in the above. For ^1H MRS acquisition, respiratory gating was not employed. Instead, breathing was paced by instruction, with a period of 4 s to synchronize with TR given to each subject prior to ^1H MRS. After a subject was trained to breathe at every 4 s to minimize breathing artifact, ^1H MRS acquisition was performed.

Both water-suppressed and non-suppressed ^1H MRS were taken in the identical voxel, and non-water suppressed spectra served as internal reference for fat quantification, as previously reported [25].

Volumes of interest (VOI's) were $3 \times 3 \times 2 \text{ cm}^3$ for liver and $2 \times 1 \times 1 \text{ cm}^3$ for pancreas. The VOI of the liver was carefully located in the posterior region of the liver, avoiding major vessels and gall bladder. The VOI of pancreas was carefully placed in the body of pancreas, avoiding visceral fat (Fig. 1c). While an automatic-shimming was employed for the liver based on FASTMAP (fast,

Fig. 1 Locations of liver fat measurements (a, b).

a Transverse MRI and a MRS voxel location. **b** Color-coded fat fraction map calculated from mDixon data. Circles in white are the regions of interest (ROIs) for fat analysis. One ROI was placed to match the MRS voxel for comparison between MRS and mDixon. Locations of pancreas fat measurements (c–e). **c** Transverse slice of mDixon MRI (fat image) with a MRS voxel location. **d** mDixon fat MRI with color-coded fat fraction map calculated from mDixon data with ROIs for fat content analysis. A larger white ROI is for processing protocol A, and a smaller pink ROI is for processing protocol B. The adjacent slice is shown in e. Typical ^1H MRS of liver and pancreas with high and low fat (f–i). **f** Liver ^1H MRS with high fat. **g** Liver ^1H MRS with low fat. The middle-chain methylene peak at 1.3 ppm is close to the baseline. **h** Pancreatic ^1H MRS with high fat. **i** Pancreatic ^1H MRS with low fat. The methylene peak at 1.3 ppm was almost undetectable



automatic shimming technique by mapping along projections) [26], an automatic shimming based on an iterative procedure was used for the pancreas, due to the smaller shim volume.

mDixon for hepatic and pancreatic fat assessment

Typical abdominal images for mDixon are depicted in Fig. 1b–e with a single breath-hold in 17 s [13, 14], using

the 16-channel SENSE coil as described above. The parameters employed for 3D fast gradient echo mDixon sequence were: flip angle = 10° , TR = 3.2 ms, TE1/TE2 = 1.12/2.0 ms, field-of-view (FOV) = $375 \times 299 \times 201 \text{ mm}^3$, acquisition matrix = $236 \times 176 \times 59$. The reconstructed 118 axial slices (1.7 mm slice thickness) of mDixon images were generated on the MRI console, as shown in Fig. 1c.

Whole body fat measurement

Whole body imaging for quantification of SAT and VAT was performed using transverse multislice turbo spin echo (TSE) sequences (TR/TE_{eff} = 400–510/38 ms) with a turbo factor of 7. These images were acquired using the quadrature body coil. The total measurement for whole body imaging took approximately 15 min. Subjects were positioned prone with extended arms and were marked on the iliac crest level, as previously reported [27].

Data processing

Hepatic and pancreatic fat quantification using ^1H MRS

Time-domain MRS data were transferred to a personal computer, processed and analyzed using the NUTS software package (Acorn NMR Inc, Livermore, CA, USA). The absolute percentage of fat content was quantified as the ratio of intensities of methylene-(CH₂)_n- (1.3 ppm) and methyl-CH₃ (0.9 ppm) peaks to the entire signal intensity [water + methylene and methyl signals] [28]. Finally, fat fraction was calculated as percentage of the ratio of [lipids/(water + lipids)] [25].

Fat quantification using mDixon

mDixon fat fraction, also expressed as lipids/(water + lipids), was obtained pixel by pixel using PRIDE software package (the version released in 2011, Philips Healthcare, Best, The Netherlands). A detailed algorithm for the PRIDE tool is given in the previous publication [14]. In brief, a two (water–fat) species model with a single fat peak assumption was employed. First, signals from 16 channels of the phased array coil were combined. A phasor for field map was assessed for each voxel by complex fitting, and then a phasor of water was estimated. Through a weighted smoothing (multiplied by magnitude mode image) in order to remove phase errors, phase errors were found and removed. After these procedures, ratios of water and fat were determined using a least square estimation. T1 or R2* correction was not included in this software. In addition, separated water and fat images were also generated.

Using the PRIDE tool, the detailed processing procedure to assess hepatic fat fractions (HFF) and pancreatic fat fractions (PFF) is as follows. Since regions of interest (ROIs) for fat content assessments were drawn post acquisition, analysis of fat content using mDixon could be analyzed using different protocols. For liver fat assessment, an ROI was placed in the same area as the voxel of the ^1H MRS measurement for comparison (Fig. 1b). In addition, to verify regional differences in the liver, three different ROI positions were selected and analyzed as shown in Fig. 1b. Three ROIs for posterior, mid, and anterior section of the liver were selected. The posterior ROI in the liver was drawn to match the corresponding VOI of ^1H MRS for fair comparison for each subject. For pancreatic fat assessment, two different processing protocols were applied. In *processing protocol A* (hereafter noted as ‘Analysis A’), ROIs were placed in several slices in the same area as the voxel of the MRS measurement to cover the VOI used in MRS, which was situated in the body of the pancreas. In the same fashion, ROIs were also placed in the tail and the head parts to assess the regional difference for Analysis A. In *processing protocol B* (hereafter noted as ‘Analysis B’), smaller ROIs were placed in three different regions of the pancreas, i. e. head, body and tail. Normally, the area of ROIs was about two to four times smaller than in Analysis A. In terms of the number of pixels, a smaller ROI in Analysis B included ~ 20 pixels, while a large ROI in Analysis A contained ~ 60 pixels. ROIs were positioned in areas where the fat level was homogenous, avoiding the borderline of the pancreas to keep contamination by visceral fat small, as shown in Fig. 1d, e (ROIs of smaller circles in pink were for Analysis B). Routinely, ROIs for Analysis B were within the ROIs for Analysis A, as shown in Fig. 1d, e in pink.

Whole body fat analysis

Whole body fat was quantified using the manual segmentation software available on the Philips MR console. Particularly, for this work, since abdominal SAT and VAT were of interest, they were assessed as abdominal SAT in the region from the diaphragm to the femoral head, and as abdominal VAT in the region (from the diaphragm to pelvis), similar to the previous publication [26].

Statistical analysis

All analyses were done using SAS for Windows Version 9.3 (SAS Institute, Cary, North Carolina, USA) All values were expressed as mean \pm standard deviation (SD). Two-sided p values less than 0.05 were considered to indicate statistically significant differences. To account for gender specific differences, we used sex-adjusted (partialized) Pearson correlations to compare VAT and SAT with HFF and PFF.

Fig. 2 Correlations and agreements between HFF by mDixon and ¹H MRS (a–b).

a Correlation between HFF by mDIXON and ¹H MRS. HFF by mDIXON was obtained in the ROIs closely matching the VOIs in MRS (correlation coefficient: $r = 0.972$, $p < 0.0001$).

b Bland–Altman plot for the two measurements. Lower and upper limits of agreement in the corresponding Bland–Altman analysis are 4.17 ± 3.22 %.

Correlations and agreements between PFF by mDixon and ¹H MRS (c–e). **c** The correlations of PFF by mDixon and ¹H MRS. Analysis A (ROIs placed to closely match the VOIs of MRS) showed better correlation with PFF by ¹H MRS ($r = 0.804$, $p < 0.0001$) than the ones from Analysis B (smaller ROIs avoiding the border of pancreas) ($r = 0.574$, $p = 0.003$).

d The Bland–Altman plot of PFF by mDixon (Analysis A) and ¹H MRS. Lower and upper limits of agreement for Analysis A are 5.56 ± 7.02 %.

e The Bland–Altman plot of PFF from mDixon (Analysis B) and ¹H MRS. Lower and upper limits of agreement for Analysis B are 2.65 ± 9.46 %, but in both analyses, the mean PFF values by mDixon are significantly higher (Analysis A: $p < 0.001$, Analysis B: $p = 0.013$) than by ¹H MRS

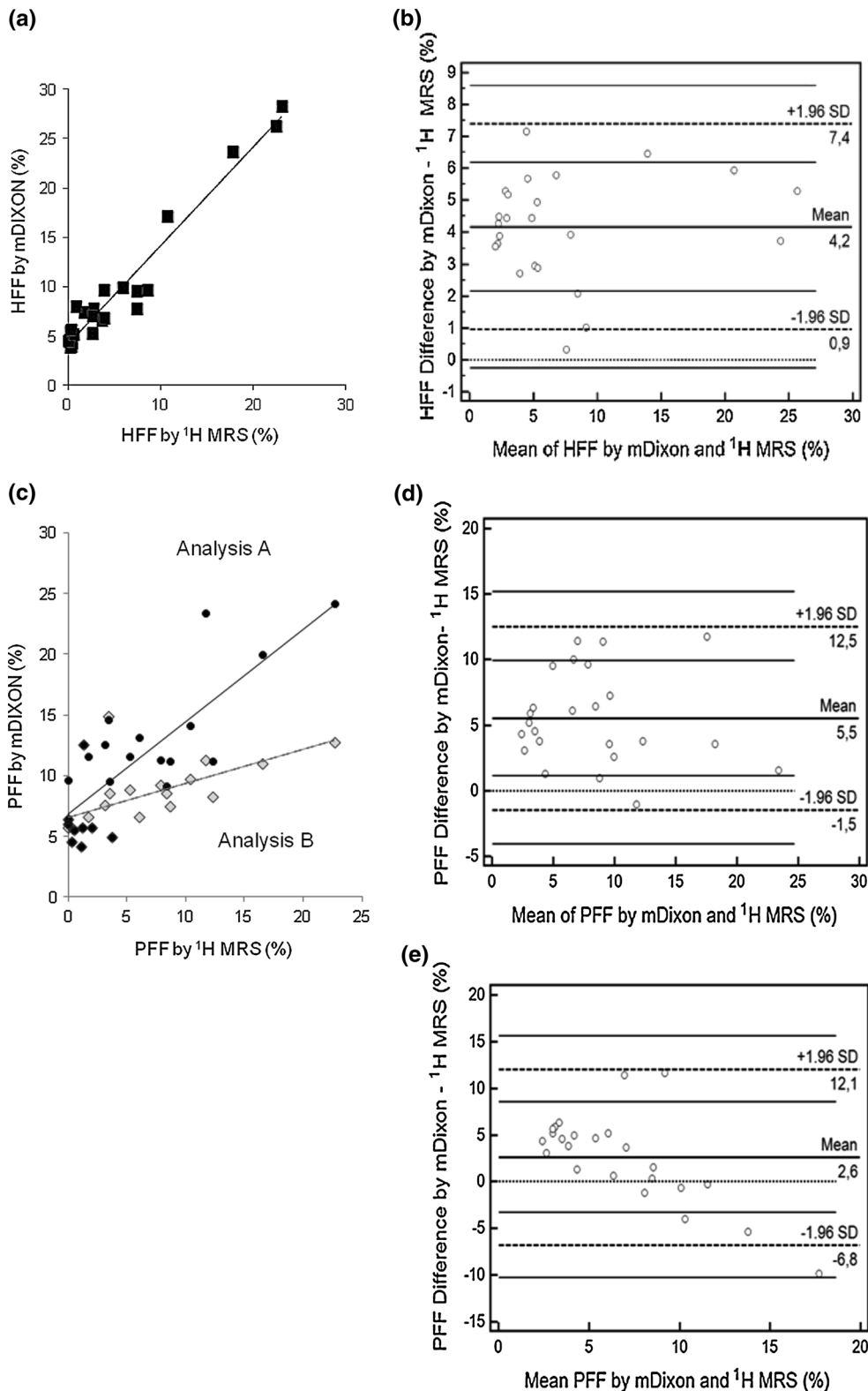


Table 1 Comparison of PFF (PFF in %) by mDIXON in three different regions in pancreas

Analysis protocol	Regional PFF in %: mean (range)		
	Head	Body	Tail
Analysis A	11.0 (3.3–28.0)	11.0 (4.2–24.2)	11.3 (3.7–19.8)
Analysis B	8.0 (3.3–14.0)	8.3 (4.2–15.0)	7.7 (3.7–12.0)

Results

Comparison of HFF using ^1H MRS and mDixon

The mean HFF was $5.32 \pm 6.83\%$ by ^1H MRS and $9.49 \pm 7.03\%$ by mDixon, when measured from areas matching locations for ^1H MRS. Values of HFF assessed with mDixon correlated with those from ^1H MRS ($r = 0.972$, $p < 0.0001$; Fig. 2a). Lower and upper limits of agreement in the corresponding Bland–Altman analysis (Fig. 2b) were $4.17 \pm 3.22\%$. The mean HFF value by mDixon was significantly higher ($p < 0.001$) than by ^1H MRS. Differences between both methods did not depend on their mean value (slope = 0.03, $p = 0.566$).

Comparison of pancreatic fat fraction (PFF) using ^1H MRS and mDixon

The mean PFF from the body of pancreas was $5.45 \pm 5.86\%$ by ^1H MRS and $11.01 \pm 5.53\%$ by mDixon using Analysis A and $8.10 \pm 2.85\%$ using Analysis B (Table 1). Since ^1H MRS was obtained from the body region of pancreas, fat values of the body region by mDixon and those by MRS were correlated as shown in Fig. 2c (Analysis A: $r = 0.804$, $p < 0.0001$; Analysis B: $r = 0.575$, $p = 0.003$; Fig. 2c). Lower and upper limits of agreement in the corresponding Bland–Altman plot for Analysis A (Fig. 2d) and B (Fig. 2e) were 5.56 ± 7.02 and $2.65 \pm 9.46\%$, respectively. In both analyses, the mean PFF value by mDixon was significantly higher (Analysis A: $p < 0.001$, Analysis B: $p = 0.013$) than by ^1H MRS. Differences between both methods did not depend on their mean value (slope = -0.06 , $p = 0.654$) in Analysis A, but they did in Analysis B (slope = -0.851 , $p = 0.0002$). The Bland–Altman plot in Analysis B suggests that PFF values by mDixon tend to larger/smaller values than those by ^1H MRS, if the mean PFF value is smaller/larger at around 9%.

Regional difference in HFF and PFF using mDixon

In this group of subjects, no statistically significant difference was found in liver fat concentration in the three examined regions; the superior frontal, mid lateral and

Table 2 Sex-adjusted (partial) Pearson correlations of hepatic and pancreatic fat contents with VAT and SAT (N = 24, 12 males and 12 females)

Organ	MR method	Correlation with adipose tissue: r (p value)	
		Abdominal VAT	Abdominal SAT
Hepatic fat	^1H MRS	0.536 (0.008)	0.375 (0.078)
	mDixon	0.490 (0.018)	0.357 (0.087)
Pancreatic fat	^1H MRS	0.605 (0.002)	0.514 (0.012)
	mDixon (Analysis B)	0.735 (<0.0001)	0.646 (0.0009)

inferior regions, but it shows a trend of HFF in the posterior section being highest (in the order of HFF in posterior > mid lateral > anterior section) ($p = 0.062$, for global test of no regional differences). Pancreatic fat content was found to be similar in head, body and tail regions (Table 1). No regional difference of fat contents within the head, body and tail of pancreas was found by employing either Analysis A ($p = 0.50$) or B ($p = 0.92$) (Table 1). Mean PFF values from Analysis A (larger ROI's) were higher by 2.9% ($p < 0.001$), 3.1% ($p < 0.002$) and 3.6% ($p < 0.001$) than those from Analysis B, in body, head and tail regions, respectively.

Relations to body fat volume

The mean abdominal volumes of VAT and SAT were 3.47 ± 2.47 liters and 5.89 ± 2.96 liters, respectively. Both HFF measured by the two methods correlated well with VAT content ($r = 0.536$, $p = 0.008$, by ^1H MRS; $r = 0.490$, $p = 0.018$, by mDixon) as in Table 2. PFF by mDixon and ^1H MRS also showed good correlations with VAT ($r = 0.605$, $p = 0.002$ by ^1H MRS; $r = 0.735$, $p < 0.0001$ by mDixon). Of note, correlations with pancreatic fat by mDixon with VAT content showed a stronger statistical significance ($p < 0.0001$ in all regions by mDixon; $p = 0.002$ by ^1H MRS in the body). Abdominal SAT showed a weaker correlation with HFF ($r = 0.375$, $p = 0.078$ by MRS; $r = 0.357$, $p = 0.0087$), but there was a stronger correlation with PFF by both ^1H MRS and mDixon as in Table 2.

Discussion

This study found that the mDixon with two flexible echo times correlated well with the gold standard ^1H MRS method for quantification of both liver and pancreas fat content. While the correlation coefficient for liver fat

measurements was close to 1.0, the correlation coefficient for pancreas fat was less tight. These overall good correlations between mDixon and ^1H MRS in liver and pancreas are consistent with previous reports for liver [8], and for both liver and pancreas using IP/OP Dixon or iterative decomposition of water and fat with echo asymmetry and least-squares estimation (IDEAL) MRI [2, 8]. The current data suggest that the fast mDixon can be utilized in clinical applications as an alternative for the more time-consuming ^1H MRS, particularly for correlative studies. However, mDixon yielded consistently higher fat values by about 3–5 % in both liver and pancreas when compared to ^1H MRS, as shown in shifted lower and upper limits of agreement by Bland–Altman analyses in results. This might be due to systematical overestimation by the current algorithm of mDixon/PRIDE software. The lower bound by ^1H MRS was lower than the one by mDixon techniques, possibly due to a higher sensitivity by ^1H MRS [4, 8]. This may currently limit the use of mDixon when aiming at detection of small changes in healthy persons with rather low HFF and PFF. Moreover, a complete removal of possible T1 weighting (by employing a lower tip angle and longer TR, or by post-acquisition corrections of T1) will further improve accurate fat quantification of mDixon method in the future. Other factors also can improve the accuracy of this mDixon method, such as T2* corrections and a multi-peak model for fat [29], which were not employed in this study, and these are other limitations of the current study.

For analysis of mDixon in pancreas, we evaluated pancreatic fat content data with two different protocols to examine VAT infiltration into the pancreatic tissue. As a result, indeed, the Analysis B (smaller ROIs) yielded slightly lower mean PFF in all three regions of pancreas.

Data from assimilated ROIs to ^1H MRS in the body region in Analysis A generated a slightly better correlation coefficient with the one by ^1H MRS ($r = 0.804$ vs. $r = 0.575$); however, the fat values of PFF from Analysis B were significantly lower. Thus, this implies that there may be more VAT infiltration near the border of the pancreas. Potential PFF values from Analysis A represent more peripancreatic fat contribution than Analysis B. However, the complex structure of the pancreas makes it difficult to separately quantify peripancreatic versus intrapancreatic fat contribution using current MRI.

Regarding possible relationships of pancreatic fat with visceral and subcutaneous fat, the present data obtained with the mDixon method showed tighter correlations in the same population than by ^1H MRS. This may suggest that PFF assessed by mDixon are more robust than the ones by ^1H MRS, probably due to less motion artifacts, even though absolute values of PFF were systematically higher. Previously, Hu et al. [2] observed that a Dixon method was more

suitable than ^1H MRS in a small organ, such as pancreas due to breathing and other motion artifact. As reported by Lingvay et al. [19], the placement of the VOI in ^1H MRS is critical in that no VAT should contaminate the VOI, which would spuriously elevate the PFF. This localization error due to the respiratory motion might have affected a high but relatively lower correlation in PFF with ^1H MRS compared to HFF in the current study. When a subject fails to cooperate with the breathing instruction, the errors in a small organ would be greater than in a big organ. According to Lingvay et al. [19], combining respiratory and cardiac gating with a smaller VOI reduced this problem of ^1H MRS.

Of note, pancreatic fat accumulation may not only result from intracellular fat storage, but also from fatty degeneration after pancreatitis. Moreover, implications of peripancreatic and intrapancreatic fat accumulation with respect to diseases have to be considered. A recent study showed that severe acute pancreatitis was strongly related to VAT, which was interpreted as increased peripancreatic fat—without directly assessing pancreatic fat [30]. At any rate, mDixon could be a good pragmatic alternative to ^1H MRS, particularly for a small organ-like pancreas, for which it would be quite difficult to employ ^1H MRS in one breath-hold. mDixon minimizes motion artifacts due to its very short acquisition time, allowing breathhold scans, and it can reduce partial volume effects of micro-regional heterogeneity of pancreas as ROIs are selected in mDixon fat maps by visual inspection. However, the clear distinction between intrapancreatic and peripancreatic fat remains difficult to achieve.

Of note, Table 1 shows that the pancreatic fat fraction is similar in the head, body and tail of the pancreas, for both analysis methods, which is also consistent with one previous publication using IP/OP Dixon [16]. This is in contrast to the hypothesis of greater fat accumulation in the pancreas tail due to the higher number of islets of Langerhans in this region [21, 31]. The fat content determined from Analysis B using smaller ROIs was lower in all the regions of the pancreas, indicating less contamination by VAT. This implies that there is heterogeneity in PFF between the peripancreas and intrapancreas.

This study also confirms the correlation between HFF and VAT [4, 20–24]. We extended this finding to the correlation between PFF and VAT, which has been reported by one [15, 21], but not other groups [18]. Moreover, we observed good and consistent correlations between PFF and VAT by two different methods, mDixon and ^1H MRS, in identical subjects (Table 2). PFF, assessed by both ^1H MRS and mDixon, correlated with both VAT and SAT, while HFF correlated with VAT, but with SAT, HFF showed only a trend.

The current data from this healthy group are probably only valid for normal and overweight, but not for severely

obese subjects. Also, patients with relevant diseases such as diabetes mellitus or pancreatitis were not studied here. Also, further studies warrant investigating detailed relations with age, sex and other factors in a large cohort in the future. In addition, we could not obtain pancreas or liver biopsy samples to validate the accuracy of the two methods, which has been previously performed at least for liver fat measurements by a similar ^1H MRS technique [32].

In summary, mDixon with 2 flexible echo times correlated well with ^1H MRS for assessing PFF and HFF with the limitations that mDixon provides a higher lower limit of detection and greater values of fat content. In addition, mDixon is a fast 3D method (144 ms/slice) that also can be employed as a good scout imaging tool for ^1H MRS for small organs, such as pancreas. Using this mDixon and ^1H MRS, PFF and HFF were consistently found to correlate with VAT and/or SAT in the same individuals. Thus, mDixon with two flexible echo times can offer a pragmatic alternative for ^1H MRS, particularly for correlative clinical studies as demonstrated in this study.

Acknowledgments The authors are grateful to the Ministry of Innovation, Science and Research (MIWFT) of the State of North Rhine-Westphalia for the installation of a 3-T whole body MR scanner at the German Diabetes Center (M. Roden). This work was supported in part by the German Federal Ministry of Education and Research (BMBF) to the German Center for Diabetes Research (DZD e.V.).

References

- Krssak M, Petersen KF, Dresner A, DiPietro L, Vogel SM, Rothman DL, Roden M, Shulman GI (1999) Intramyocellular lipid concentrations are correlated with insulin sensitivity in humans: a ^1H NMR spectroscopy study. *Diabetologia* 42:113–116
- Hu HH, Nayak KS, Goran MI (2010) Assessment of abdominal adipose tissue and organ fat content by magnetic resonance imaging. *Obesity* 18:841–847
- Thomsen C, Becker U, Winkler K (1994) Quantification of liver fat using magnetic resonance spectroscopy. *Magn Reson Imaging* 12:487–495
- Sijens PE, Edens MA, Bakker SJL, Stolk RP (2010) MRI-determined fat content of human liver, pancreas and kidney. *World J Gastroenterol* 28(16):1993–1998
- Szczepaniak LS, Nurenberg P, Leonard D, Browning JD, Reingold JS, Grundy S, Hobbs HH, Dobbins RL (2005) Magnetic resonance spectroscopy to measure hepatic triglyceride content: prevalence of hepatic steatosis in the general population. *Am J Physiol Endocrinol Metab* 288:E462–E468
- Dixon WT (1984) Simple proton spectroscopic imaging. *Radiology* 153:189–194
- Ma J (2008) Dixon techniques for water and fat imaging. *J Magn Reson Imaging* 28:543–558
- Kim H, Taksali SE, Dufour S, Befroy D, Goodman TR, Petersen KF et al (2008) A Comparative MR study of hepatic fat quantification using single-voxel proton spectroscopy, two-point Dixon and three-point IDEAL. *Magn Reson Med* 59(3):521–527
- Ma X, Holalkere NS, Kambadakone AR, Kenudson MN, Hahn PF, Sahani DV (2009) Imaging-based quantification of hepatic fat: methods and clinical applications. *Radio Graphics* 29:1253–1280
- Xiang QS (2006) Two-point water–fat imaging with partially-opposed-phase (POP) acquisition: an asymmetric Dixon method. *Magn Reson Med* 56:572–584
- Reeder SB, Wen Z, Yu H, Pineda AR, Gold GE, Markl M, Pelc NJ (2004) Multicoil Dixon chemical species separation with an iterative least squares estimation method. *Magn Reson Med* 51:35–45
- Ma J (2004) Breath-hold water and fat imaging using a dual-echo two-point Dixon technique with an efficient and robust phase-correction algorithm. *Magn Reson Med* 52:415–419
- Eggers H, Brendel B, Duijndam A, Herigault G (2011) Dual-echo Dixon imaging with flexible choice of echo times. *Magn Reson Med* 65:96–107
- Berglund J, Ahlström H, Johansson L, Kullberg J (2011) Two-point Dixon method with flexible echo times. *Magn Reson Med* 65:994–1004
- van Raalte DH, van der Zijl NJ, Diamant M (2010) Pancreatic steatosis in humans: cause or marker of lipotoxicity? *Curr Opin Clin Nutr Metab Care* 13:478–485
- Heni M, Machann J, Staiger H, Schwenzer NF, Peter A, Schick F, Claussen CD, Stefan N, Häring HU, Fritsche A (2010) Pancreatic fat is negatively associated with insulin secretion in individuals with impaired fasting glucose and/or impaired glucose tolerance: a nuclear magnetic resonance study. *Diabetes Metab Res Rev* 26(3):200–205
- Schwenzer NF, Machann J, Martirosian P, Stefan N, Schraml C, Fritsche A, Claussen CD, Schick F (2008) Quantification of pancreatic lipomatosis and liver steatosis by MRI: comparison of in/opposed-phase and spectral–spatial excitation techniques. *Invest Radiol* 43:330–337
- Tushuizen ME, Bunck MC, Pouwels PJ, Bontemps S, van Waesberghe JH, Schindhelm RK et al. (2007) Pancreatic fat content and β -cell function in men with and without Type 2 diabetes. *Diabetes Care* 30:2916–2921
- Lingvay L, Esser V, Legendre JL, Price AL, Wertz KM, Adams-Huet B, Zhang S, Unger RH, Szczepaniak LS (2009) Noninvasive quantification of pancreatic fat in humans. *J Clin Endocrinol Metab* 94:4070–4076
- van der Zijl NJ, Goossens GH, Moors CCM, van Raalte DH, Muskiet MHA, Pouwels PJW, Blaak EE, Diamant M (2011) Ectopic fat storage in the pancreas, liver, and abdominal fat depots: impact on cell function in individuals with impaired glucose metabolism. *J Clin Endocrinol Metab* 96:459–467
- Le KA, Ventura EE, Fischer JQ, Weigensberg MJ, Punyanitya M, Hu HH, Nayak KS, Goran MI (2011) Ethnic differences in pancreatic fat accumulation and its relationship with other fat depots and inflammatory markers. *Diabetes Care* 34:485–490
- Kovanlikaya A, Mittelman SD, Ward A, Geffner ME, Dorey F, Gilsanz V (2005) Obesity and fat quantification in lean tissues using three-point Dixon MR imaging. *Pediatr Radiol* 35:601–607
- Nguyen-Duy EB, Nichaman MZ, Church TS, Steven N (2003) Visceral fat and liver fat are independent predictors of metabolic risk factors in men. *Am J Physiol Endocrinol Metab* 284:E1065–E1071
- Hwang J-H, Stein DT, Barzilay N, Cui M-H, Tonelli J, Kishore P, Hawkins M (2007) Increased intrahepatic triglyceride is associated with peripheral insulin resistance: in vivo MR imaging and spectroscopy studies. *Am J Physiol Endo Metab* 293:E1663–E1669
- Machann J, Thamer C, Schnoedt B, Stefan N, Häring H-U, Claussen CD, Fritsche A, Schick F (2006) Hepatic lipid accumulation in healthy subjects: a comparative study using spectral

- fat-selective MRI and volume-localized ^1H -MR spectroscopy. *Magn Reson Med* 55:913–917
26. Gruetter R (1993) Automatic, localized in vivo adjustment of all first- and second-order shim coils. *Magn Reson Med* 29:804–811
 27. Machann J, Thamer C, Stefan N, Schwenzer NF, Kantartzis K, Häring H-U, Claussen CD, Fritsche A, Schick F (2010) Follow-up whole-body assessment of adipose tissue compartments during a lifestyle intervention in a large cohort at increased risk for type 2 diabetes. *Radiology* 2:353–363
 28. Hamilton G, Yokoo T, Bydder M, Cruite I, Schroeder ME, Sirlin CB, Middleton MS (2011) In vivo characterization of the liver fat ^1H MR spectrum. *NMR Biomed* 24:784–790
 29. Hu HH, Börnert P, Hernando D, Kellman P, Ma J, Reeder S, Sirlin C (2012) ISMRM workshop on fat–water separation: insights, applications and progress in MRI. *Magn Reson Med* 68(2):378–388
 30. Yashima Y, Isayama H, Tsujino T, Nagano R, Yamamoto K, Mizuno S, Yagioka H, Kawakubo K, Sasaki T, Kogure H, Nakai Y, Hirano K, Sasahira N, Tada M, Kawabe T, Koike K, Omata M (2011) A large volume of visceral adipose tissue leads to severe acute pancreatitis. *J Gastroenterol* 46:1213–1218
 31. Netter FH (1970) *The CIBA collection of medical illustrations: endocrine system and selected metabolic diseases*. CIBA, New York
 32. Krssák M, Hofer H, Wrba F, Meyerspeer M, Brehm A, Lohninger A, Steindl-Munda P, Moser E, Ferenci P, Roden M (2010) Non-invasive assessment of hepatic fat accumulation in chronic hepatitis C by ^1H magnetic resonance spectroscopy. *Eur J Radiol* 74:e60–e66. doi:[10.1016/j.ejrad.2009.03.062](https://doi.org/10.1016/j.ejrad.2009.03.062)